Tentative Mechanism for the Bistability Observed during Irradiation of the Triphenylimidazolyl Radical Dimer in a CSTR

B. Borderie,[†] D. Lavabre,[†] G. Levy,[†] J. C. Micheau,[†] and J. P. Laplante*[,‡]

Contribution from the Laboratoire des IMRCP, UA au CNRS No. 470, Université Paul Sabatier, 31062 Toulouse, France, and the Department of Chemistry and Chemical Engineering, Royal Military College of Canada, Kingston, Ontario, Canada K7L 5L0. *Received September 21, 1989*

Abstract: We previously reported on the observation of a bistability when a chloroform solution of the triphenylimidazolyl radical dimer (TPID) is irradiated in a CSTR (continuous flow stirred tank reactor) (*J. Phys. Chem.* **1988**, *92*, 16). In the present paper, the photochemistry of TPID in chloroform is examined in more detail and key reactions are summarized in a 6-step mechanism. Values of relevant kinetic parameters are determined and used in numerical simulations of the TPID/$CHCl_3$ photochemistry in a CSTR. Multiple steady states are indeed observed when experimental values of the kinetic parameters are used in the simulations. The bistability width and transition points are in good agreement with experimental results. It is suggested that the feedback mechanism responsible for the instability is of photometric origin. One of its key components is the screen effect that arises as the result of competitive absorption in multicomponent photochemical systems.

We recently reported on the observation of a bistability when a chloroform solution of the triphenylimidazolyl radical dimer (TPID, **1**; Figure 1) is irradiated in a continuous flow stirred tank reactor (CSTR).[1,2] When the reactor is open to a flow of TPID, two distinct stable steady states can be obtained for the same set of external constraints (Figure 2). In the upper state (flow branch), the solution is reddish purple, indicating a high concentration of triphenylimidazolyl radicals (TPI•, **2**; Figure 1). The lower state is on the other hand characterized by a strong fluorescence and an almost complete disappearance of TPI• radicals. Previous high-pressure liquid chromatography (HPLC) studies have confirmed the presence of the 2,4,5-triphenylimidazole (TPI, **3**; Figure 1) as one of the intermediate products of the photoreaction.[1,2] Photolysis of TPI produces a variety of photoproducts,[3,4] one of which was identified as the 2-phenyl-9,10-phenanthroimidazole, a strongly fluorescent compound (PPI, **4**; Figure 1).[1,2] This compound is believed to be responsible for the strong blue fluorescence observed in the lower absorbance state.

In our first report, we briefly presented a qualitative mechanism to account for the observed experimental bistability.[1] The origin of the instability was suggested to lie in the competitive absorption of light by the various species. A theoretical study of the A ($+h\nu$) $\rightleftarrows$ B ($+h\nu$) $\rightarrow$ C model system (hereafter referred to as the ABC model) did indeed show that competitive light absorption can give rise to multiple steady states.[5] The TPID/$CHCl_3$ photochemistry is, however, much more complex than the minimal ABC model. It is therefore doubtful that one could quantitatively account for our CSTR results[1,2] in terms of such a simple model. In the present paper, we go one step further in our understanding of the TPID bistability and present a more detailed and quantitative analysis of the TPID/$CHCl_3$ photochemistry. The bulk of the available information on the TPID/$CHCl_3$ photochemistry is summarized in a 6-step reaction mechanism. The experimental determination of relevant kinetic parameters is discussed, and these parameters are used in numerical simulations of the photoreaction dynamics in a CSTR. Bistability is obtained in the simulations when experimental values of the kinetic parameters are used. Transition points and the bistability width are in good agreement with the experimental bistability. The nature of the feedback mechanism leading to the instability is discussed.

Experimental Section

TPID was prepared from commercial 2,4,5-triphenylimidazole (Lophine, Aldrich T8, 320-8, TPI, Figure 1) according to the procedure of White and Sonnenberg.[6] This procedure gives the TPID piezodimer in excellent yield (>95%). Solutions of the corresponding photochromic dimer used in our experiments were obtained by merely dissolving the piezodimer in chloroform and leaving the solution in the dark for approximately 30 min. As the piezodimer is added to chloroform, a deep violet color due to the triphenylimidazolyl radical monomer (TPI•, Figure 1) is first observed. On standing in the dark this color slowly fades, as the radicals recombine to give the photochromic TPID. As this takes place, a significant fraction of TPI• radicals is converted to TPI through hydrogen abstraction from the chloroform solvent.[4a] This side reaction is here unavoidable, and as a result, the TPID/$CHCl_3$ solutions contain up to 15% TPI (determined by high pressure liquid chromatography). The flow reactor experiments shown in Figure 2 were done in a 1.10-mL quartz CSTR, the design of which has been described elsewhere.[1,2,11] Batch runs were also carried out in the same reactor. Irradiation was carried out with a 200-W high-pressure mercury lamp, through a 360-nm bandpass filter. In all experiments, spectroscopic grade chloroform was used as the solvent. This solvent contains 0.8% ethanol as a stabilizing agent. All solutions were purged with nitrogen for 10 min before use and kept under a nitrogen atmosphere thereafter. Absorption spectra of TPID and TPI were recorded on a Beckman M IV spectrophotometer (determination of ϵ_{360}^{TPID} and ϵ_{360}^{TPI}). In the CSTR experiments, non-irradiated solutions of TPID in chloroform were used as the reference. Since the TPI• radical is the only species absorbing significantly at 554 nm (λ_{max}), this wavelength was chosen as the monitoring wavelength. The diode array detection used in conjunction with our CSTR allows the whole UV-vis spectrum to be recorded as a function of time. High-pressure liquid chromatography (HPLC) analysis was carried out with a C_{18}-μ-Bondapack reverse-phase HPLC column (Waters). The mobile phase was CH_3OH/H_2O, 85/15 (% v/v).[2]

Results and Discussion

A. The Photochemistry of TPID in Chloroform. The purpose of this section is twofold: (a) present evidence to support the set of reactions (R1-R6) as a skeleton mechanism for the photo-

[†] Université Paul Sabatier.
[‡] Royal Military College of Canada.

(1) Lavabre, D.; Levy, G.; Laplanie, J. P.; Micheau, J. C. *J. Phys. Chem.* **1988**, *92*, 16-18.
(2) Levy, G.; Lavabre, D.; Micheau, J. C.; Laplante, J. P. *New J. Chem.* **1988**, *12*, 839-846.
(3) (a) Hennessy, J.; Testa, A. C. *J. Phys. Chem.* **1972**, *76*, 3362-3365. (b) Takach, P.; Testa, A. C. *J. Photochem.* **1987**, *22*, 285-290.
(4) (a) Maeda, K.; Hayashi, T. *Bull. Chem. Soc. Jpn.* **1970**, *43*, 429-438. (b) Sakaino, Y.; Kakisawa, H.; Arita, K.; Kouno, M.; Morishima, H. *Tetrahedron* **1973**, *29*, 1185-1191.
(5) Laplante, J. P.; Lavabre, D.; Micheau, J. C. *J. Chem. Phys.* **1988**, *89*, 1435-1442.
(6) White, D. M.; Sonnenberg, J. *J. Am. Chem. Soc.* **1966**, *88*, 3825-3829.
(7) Pickering, M. *J. Chem. Educ.* **1980**, *57*, 833-834.
(8) Kornblum, N. *Angew. Chem., Int. Ed. Engl.* **1975**, *14*, 734-745 and references therein.
(9) Murov, S. L. *Handbook of Photochemistry*; Marcel Dekker: New York, 1973; Section 13.
(10) Johnson, K. J. *Numerical Methods in Chemistry*; Marcel Dekker: New York, 1980.
(11) Grégoire, F.; Gimenez, M.; Lavabre, D.; Laplante, J. P.; Micheau, J. C. *J. Photochem.* **1985**, *28*, 261-271.
(12) Borderie, B.; Lavabre, D.; Levy, G.; Micheau, J. C.; Laplante, J. P. *React. Kin. Catal. Lett.* To be published.

0002-7863/90/1512-4105$02.50/0

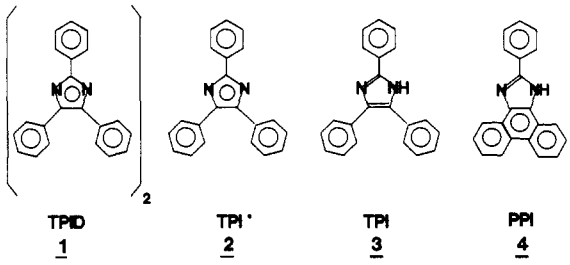

Figure 1. Chemical structures of the main species involved in the photochemistry of the triphenylimidazolyl radical dimer in chloroform.

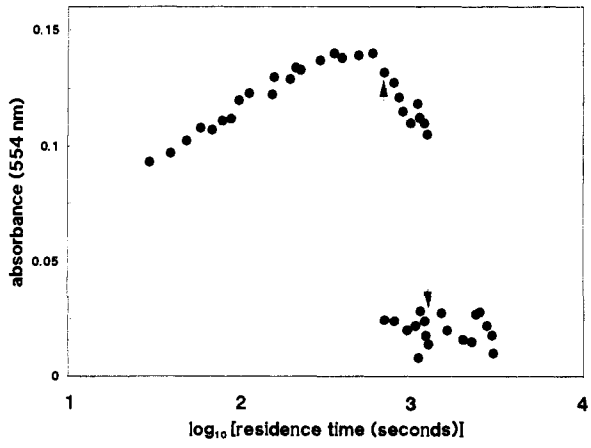

Figure 2. Photostationary absorbances of irradiated TPID/$CHCl_3$ solutions as a function of the residence time in a 1.10-mL CSTR. The absorbance at 554 nm is directly proportional to the TPI• radical concentration. $[TPID]_0 = 5.0 \times 10^{-4}$ M, $[TPI]_0 = 9.0 \times 10^{-5}$ M, $I_0 = 1.43 \times 10^{-4}$ M·s^{-1}, where $[\,]_0$ refers to concentrations in the reactor before any reaction takes place. Note that the absorbance scale corresponds to the 1.5 mm path length flow-through cell used in the diode array detection system. This cell is located a few centimeters down the outflow point of the CSTR. The path length of the irradiated cell itself is 1 cm.

chemistry of TPID in chloroform and (b) discuss the kinetic parameters required to quantitatively describe the system's dynamics.

$$\text{TPID} \xrightarrow{h\nu} 2\text{TPI}^{\bullet} \qquad \text{(R1)}$$

$$\text{TPI}^{\bullet} \xrightarrow[CHCl_3]{} \text{TPI} \qquad \text{(R2)}$$

$$2\text{TPI}^{\bullet} \rightarrow \text{TPID} \qquad \text{(R3)}$$

$$\text{TPI} \xrightarrow{h\nu} \text{PPI} \qquad \text{(R4)}$$

$$\text{TPI} \xrightarrow[CHCl_3]{h\nu} H^+ + \text{TPI} \qquad \text{(R5)}$$

$$\text{TPI}^{\bullet} + H^+ \xrightarrow[\text{electron donor}]{} \text{TPI} \qquad \text{(R6)}$$

Reaction R1. This photoreaction corresponds to the homolytic fission of the TPID dimer into its radical moieties. It is the reaction responsible for the TPID photochromism. This reaction was first discovered by White and Sonnenberg[6] and later studied by Maeda and Hayashi.[4] In a stirred reactor, the rate of production of TPI• radicals through process R1 can be written as

$$r_1 = \phi_1 I_1 \qquad (1)$$

where ϕ_1 is the quantum yield of reaction R1 and I_1 the amount of light absorbed by TPID at the irradiation wavelength (360 nm). With use of Beer's law and assuming a unit path length, I_1 can be written as

$$I_1 = I_0 \frac{(1 - 10^{-A_{360}})}{A_{360}} \epsilon_{360}[\text{TPID}] \qquad (2)$$

where I_0 is the incident light flux at the front face of the cell and A_{360} is the total absorbance at the irradiation wavelength. Assuming that TPID, TPI•, and TPI are the only species absorbing significantly at 360 nm, the total absorbance at that wavelength is given by

$$A_{360} = \epsilon_{360}^{\text{TPID}}[\text{TPID}] + \epsilon_{360}^{\text{TPI}^{\bullet}}[\text{TPI}^{\bullet}] + \epsilon_{360}^{\text{TPI}}[\text{TPI}] \qquad (3)$$

where ϵ_{360}^{i} is the molar extinction coefficient of species "i" at the irradiation wavelength. Expressions 1–3 contain a number of kinetic and spectroscopic parameters, the values of which had to be determined. Their determination is described in Appendix A and a summary of experimental values can be found in Table I.

Table I. Spectroscopic and Kinetic Parameters for the TPID/$CHCl_3$ Photoreaction

$\epsilon_{360}^{\text{TPID}}$,[a] L·mol^{-1}·cm^{-1}	1850
$\epsilon_{360}^{\text{TPI}^{\bullet}}$,[a] L·mol^{-1}·cm^{-1}	37000
$\epsilon_{360}^{\text{TPI}}$,[a] L·mol^{-1}·cm^{-1}	570
$\epsilon_{554}^{\text{TPID}}$, L·mol^{-1}·cm^{-1}	0
$\epsilon_{554}^{\text{TPI}^{\bullet}}$,[a] L·mol^{-1}·cm^{-1}	7000
$\epsilon_{554}^{\text{TPI}}$, L·mol^{-1}·cm^{-1}	0
ϕ_1	0.013 ± 0.008
ϕ_4	0.0012 ± 0.0005
ϕ_5	0.009 ± 0.003
I_0, M·s^{-1}	$(1.43 \pm 0.1) \times 10^{-4}$
k_2, L·mol^{-1}·s^{-1}	$(6.0 \pm 0.5) \times 10^{-4}$
k_3, L·mol^{-1}·s^{-1}	10 ± 1
k_6, L·mol^{-1}·s^{-1}	524 ± 50

[a] These values were obtained in chloroform solutions and differ slightly from the ones used in ref 1.

Reaction R2. This reaction corresponds to the thermal degradation of TPI• radicals through hydrogen abstraction from the solvent.[4] The corresponding first-order rate constant, k_2, was determined from a kinetic study of the decay rate of TPI• radicals at the very beginning of the photoreaction (Appendix A; Table I). According to Maeda and Hayashi,[4] oxidation of TPI• radicals with dissolved oxygen can also take place in solution. Since all our batch and flow reactor experiments were done with nitrogen-purged solutions, this reaction is here believed to be much less significant than (R2) and is therefore neglected.

Reaction R3. Reaction R3 corresponds to the bimolecular recombination of TPI• radicals to regenerate TPID. Its rate constant in benzene, k_3, was previously found to be 66 L·mol^{-1}·s^{-1} at 25 °C.[4a] From a kinetic study of the decay curves in chloroform we find a somewhat lower value, 10 L·mol^{-1}·s^{-1}, at the same temperature (Appendix A; Table I).

Reaction R4. The photolysis of phenylimidazoles was initially studied by Hennessy and Testa.[3] In outgassed solutions, these authors identified the main photoproduct as the 2-phenyl-9,10-phenanthroimidazole (PPI), a strongly fluorescent compound.[3] Previous HPLC studies have confirmed the presence of PPI as a major photoproduct of the photolysis of TPID in chloroform.[1,2] The rate of production of PPI through process R4 can be written as

$$r_4 = \phi_4 I_4 \qquad (4)$$

where ϕ_4 is the quantum yield of reaction R4 and I_4 is the amount of light absorbed by TPI. As in eq 2, one can write

$$I_4 = I_0 \frac{(1 - 10^{-A_{360}})}{A_{360}} \epsilon_{360}^{\text{TPI}}[\text{TPI}] \qquad (5)$$

where A_{360} has already been defined in eq 3. The quantum yield ϕ_4 was determined from a quantitative study of the photolysis of solutions of TPI in chloroform (Appendix A). Our value of $\phi_4 = 0.0012$ compares well with the one found by Hennessy and Testa, i.e. 0.0022 (in ethanol).[4a]

Reaction R5. Early in our study of the TPID/$CHCl_3$ photochemistry it was noted that the reaction photoproducts were efficient scavengers of TPI• radicals. The scavenging is believed to occur through an acid produced in one of the photoreactions. The amount of acid produced was measured for increasing irradiation times in batch runs, by titrating the irradiated TPID/

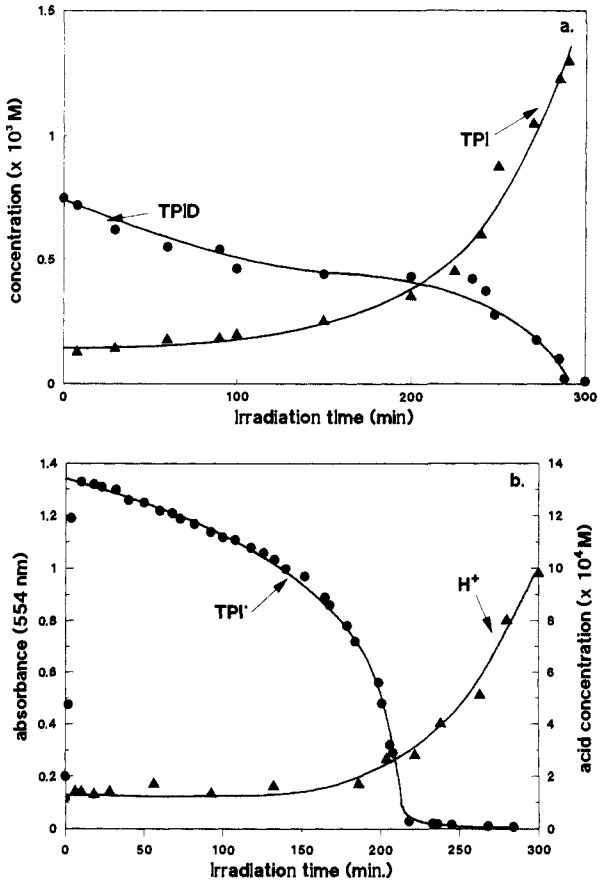

Figure 3. (a) Time evolution of TPID and TPI concentrations in a batch experiment, under irradiation at 360 nm. $[TPID]_0 = 7.5 \times 10^{-4}$ M, $[TPI]_0 = 1.8 \times 10^{-5}$ M. Concentrations were determined by HPLC, for increasing irradiation times. (b) Time evolution of H^+ and TPI• radicals, under conditions of part a. Acid concentrations were determined by titrating the irradiated solutions with KOH. TPI• concentrations were determined from Beer's law, using data of Table I.

$CHCl_3$ solutions with ethanolic solutions of KOH. The results are shown in Figure 3b along with the corresponding TPI• concentrations. Comparing parts a and b of Figure 3 suggests that the acid is formed in parallel with TPI. One possibility is that the acid is produced via the TPI-sensitized photolysis of chloroform solvent (reaction R5).[13] The rate of formation of H^+ through (R5) can be written as[13]

$$r_5 = \phi_5 I_4 \qquad (6)$$

where ϕ_5 is the quantum yield of acid formation and I_4 is as defined previously in eq 5. Quantum yield ϕ_5 was determined from a quantitative analysis of the rate of formation of acid in irradiated solutions of TPID in chloroform (Appendix A).

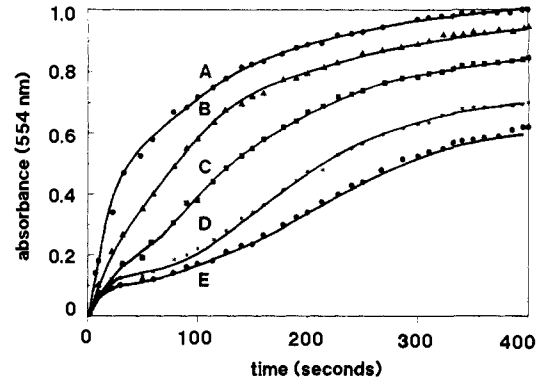

Figure 4. Effect of increasing amounts of acid added to the TPID/$CHCl_3$ photoreaction on the rate of formation of TPI• radicals. The concentrations of monochloroacetic acid added (M) for each of the runs shown above were (A) 0, (B) 6.5×10^{-8}, (C) 1.3×10^{-7}, (D) 1.9×10^{-7}, and (E) 2.6×10^{-7}. The acid was added quantitatively, before the irradiation was turned on. Irradiation conditions were as the same as for Figure 2.

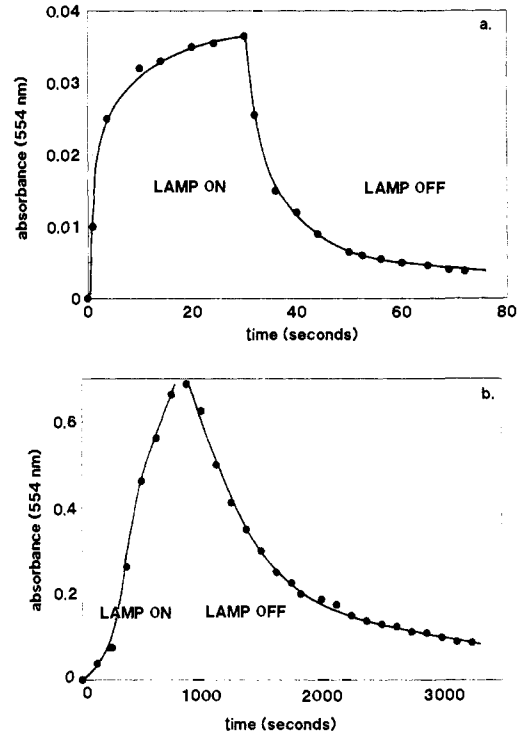

Figure 5. Qualitative comparison of the decay rate of TPI• radicals (a) early in the irradiation versus (b) much later in the irradiation. The conditions were the same as for Figure 4, curve E. Note the difference in absorbance and time scales between (a) and (b).

Reaction R6. This process corresponds to the quenching of TPI• radicals by the acid formed in reaction R5. The quenching effect of the acid on TPI• radicals is illustrated in Figure 4. In that series of experiments, controlled amounts of monochloroacetic acid were added to TPID/$CHCl_3$ solutions, *before irradiation*. As seen in Figure 4, the rate of formation of TPI• radicals decreases significantly in the presence of acid. For the larger concentrations of added acid, a plateau is clearly seen to be reached early in the irradiation. Two possible mechanisms through which H^+ could quench TPI• radicals are (a) quenching of the TPID excited state leading to the formation of TPI• radicals or (b) bimolecular reaction of TPI• radicals with H^+. If the first mechanism was operative, the decay rate of TPI• radicals should be independent of the irradiation time. As seen in Figure 5, this is not the case. If the irradiation is stopped during the plateau, i.e. while the concentration of acid is still high, the TPI• radical concentration

(13) It is well-known that $CHCl_3$ is light-sensitive and can photolyze through radical chain processes.[14-16] The dissociation energy of $CHCl_3$ into CCl_2 and HCl is of the order of 2.52 eV (492 nm).[17] However, chloroform does not absorbe at that wavelength. Its decomposition can, however, be photosensitized. One of the possible sensitizers is TPI. Photosensitization could take place through energy transfer

$$TPI^* + CHCl_3 \rightarrow TPI + CHCl^*_3$$

$$CHCl^*_3 \rightarrow CCl_2 + HCl$$

or alternatively through chemical photosensitization:

$$TPI^* + CHCl_3 \rightarrow TPIH^{\cdot} + CCl_3^{\cdot} \text{ (solvent cage)}$$

$$CCl_3^{\cdot} + CHCl_3 \rightarrow CCl_2 + HCl + CCl_3^{\cdot}$$

$$TPIH^{\cdot} + CCl_3^{\cdot} \rightarrow TPI + CHCl_3$$

(14) Ogita, T.; Hatta, H.; Hiroshi, N.; Sei, I.; Kagiya, T. *Nippon Kagaku Kaishi* **1985**, *5*, 970–975.
(15) Ogita, T.; Hatta, H.; Kagiya, T. *Kankyo Gijutsu* **1983**, *12*, 370–372.
(16) Benrath, A. *Annalen* **1911**, *382*, 222–235.
(17) Kenner, R. D.; Haak, H. K.; Stuhl, F. *J. Chem. Phys.* **1986**, *85*, 1915–19.

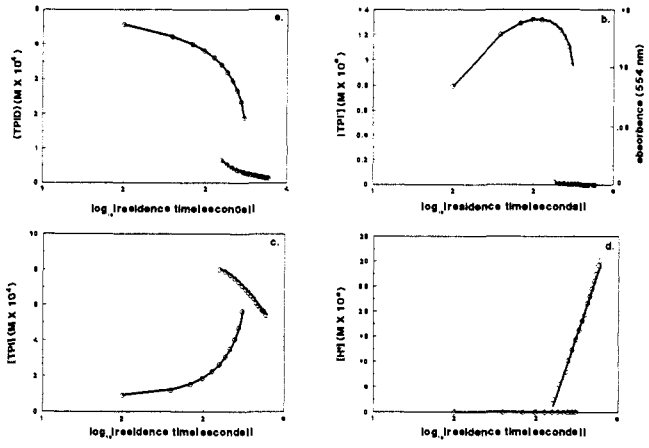

Figure 6. Steady states of the system of eq 7 for experimental values of parameters given in Table I. As in Figure 2, the steady states are plotted as a logarithmic function of the residence time in the CSTR. The right-hand scale in Figure 6b corresponds to the 554-nm absorbances that would be observed for a 1.5 mm detection path length. This path length corresponds to the one used in our experimental detection system (see Figure 2).

decreases rapidly (Figure 5a). If, on the other hand, the irradiation is turned off after a longer irradiation time the decay is much slower (Figure 5b). A titration of TPI• radicals with monochloroacetic acid indicates a 1:1 stoichiometry for the quenching reaction. We therefore suggest that the quenching occurs through a bimolecular reaction between TPI• radicals and H^+, followed by an electron transfer. This electron transfer could occur through $CHCl_3$ or via one of the heterocycles present in solution.[8] As a result, TPI is regenerated in reaction R6. The rate for this process, k_6, was estimated from the decay rate of TPI• radicals in acidic solutions (Appendix A; Table I).

B. The Steady States. In this section, we examine the photostationary states of the system of reactions R1–R6 when carried out in a CSTR. Assuming the reactor to be fed with TPID and TPI at a rate k_0 and concentrations $[TPID]_0$ and $[TPI]_0$, the rate equations are written as (eqs 1–6)

$$d[TPID]/dt = -r_1/2 + 2k_3[TPI^\bullet]^2 + k_0\{[TPID]_0 - [TPID]\}$$

$$d[TPI^\bullet]/dt = r_1 - 2k_3[TPI^\bullet]^2 - (k_2 + k_0)[TPI^\bullet] - k_6[H^+][TPI^\bullet]$$

$$d[TPI]/dt = -r_4 + k_2[TPI^\bullet] + k_6[TPI^\bullet][H^+] + k_0\{[TPI]_0 - [TPI]\}$$

$$d[H^+]/dt = r_5 - k_6[TPI^\bullet][H^+] - k_0[H^+] \quad (7)$$

where rate expressions r_1, r_4, and r_5 have been defined previously in eqs 1–6. The system of eq 7 was solved numerically with a fourth-order Runge–Kutta algorithm.[10] Figure 6 shows the system's steady states for values of parameters corresponding to the experimentally determined values (Table I). To facilitate the comparison with Figure 2, steady-state concentrations are here plotted as a function of the residence time, k_0^{-1}. In the present work, no systematic attempt was made to fit the model to the experimental results. Given the large number of parameters and the known sensitivity of the related ABC model to parameter variation,[5] it is encouraging to find that bistability is indeed obtained in the model when experimental values are used. The shapes of both high and low TPI• concentration branches in Figure 6b are very similar to the high and low absorbance branch observed experimentally (Figure 2). The bistability width as well as the location of both transition points are also in good qualitative agreement with experimental results. The system of reactions R1–R6 is therefore believed to constitute a good first approximation to the photochemistry of TPID in chloroform.

The feedback responsible for the observation of multiple steady states is here believed to be of photometric origin. This type of feedback is unique to multicomponent photochemical systems and is more or less hidden in the nonlinear dependency of photochemical rates on concentration variables. One of its key components is the *screen effect* that arises as the result of competitive light absorption. In order to clarify the role of the screen effect in the photometric feedback, let us first emphasize that in photochemical systems, the rate at which a given photochemical reaction takes place is governed by Beer's law.[5] As an example, let us consider the irreversible photodegradation of TPI to PPI, reaction R4. As shown in the previous section (eqs 3–5), the photochemical rate r_4 depends not only on the TPI concentration but as well on the concentration of the other light absorbers such as TPID and TPI• radicals. The latter can therefore be thought of as acting as a screen to the TPI ($+h\nu$) → PPI photoreaction: the higher their concentration, the slower the photoreaction will be. The *photometric* feedback responsible for the instability arises as the result of the coupling of the screen effect with reactions R5 and R6. In reaction R5, TPI acts as a photosensitizer for the production of acid H^+. Because of the screen effect, (R5) remains slow as long as the concentrations of TPID and TPI• radicals are high (short residence times). Since $\epsilon_{360}^{TPI^\bullet} \gg \epsilon_{360}^{TPI}$, this screen is particularly efficient in controlling the rate of reaction R5. As the steady-state concentration of TPI• radicals decreases, the screen effect is weakened and as a result more light becomes available to the weak absorber TPI for the photosensitized production of acid. The rate at which H^+ is produced in (R5) and at which TPI• radicals are destroyed in (R6) therefore increases. The concurrent decrease in the TPI• radical concentration further weakens the screen effect that leads to an increase in the rate of (R5) and (R4). In a batch reactor, this photometric feedback leads to an autocatalytic-like time dependency for both TPI and H^+ concentrations (Figure 3a,b). In a CSTR, it leads to multiple steady states.

On the basis of the above mechanism, the observation of multiple steady states in the $TPID/CHCl_3$ system can now be understood as follows. At very short residence times, processes R2 and R3 compete efficiently with the photoproduction of TPI• radicals through (R1). As the residence time increases, more radicals are produced and therefore [TPI•] increases rapidly until a maximum is reached (figure 6b). As this takes place, the TPID concentration decreases slightly (Figure 6a). At these short residence times, process R2 essentially governs the steady-state concentration of TPI (Figure 6c), and very little irreversible photochemistry is taking place. What is observed is essentially the reversible photochromism of TPID. As the residence time is increased, a larger and larger fraction of the incoming light flux becomes available to TPI for the photosensitized production of acid. As the steady-state concentration of TPI• radicals decreases the screen effect weakens, which leads to a further increase in the rate of acid production. Beyond a critical residence time, the rate of formation of TPI• radicals through (R1) is no longer large enough to maintain the system on the high absorbance branch. A transition to a much lower absorbance state is then observed as one increases the residence time beyond that critical point. The low absorbance branch is characterized by a negligible concentration of TPI• radicals. The rate of reaction R6 is therefore very small, which allows the steady-state concentration of acid to increase steadily as one further increases the residence time (Figure 6d). Destabilization of the lower branch occurs when the flow rate becomes large enough to compete efficiently with (R6). Since this destabilization mechanism is different from the one operative in the high absorbance branch, the transition from low to high absorbance states takes place at a different residence time, hence hysteresis.

As a final note, let us add that a preliminary study of the effect of various parameters on the model bistability reveals a pattern similar to what was found in the much simpler ABC model.[5] For example, bistability disappears if the irradiation intensity I_0 is either too high or too low. This parameter was found to be very critical in our earlier attempts to reproduce our original experimental results.[1] On the other hand, our simulations suggest that the bistability is relatively insensitive to minor variations in the concentration of TPI in the TPID flow. Changing $[TPI]_0$ by 10

to 20% does not affect the width of the bistability significantly. Work is presently in progress to verify experimentally some of the model predictions.

Conclusion

In this paper, we have presented a tentative mechanism to account for the multiple steady states observed when a TPID/$CHCl_3$ solution is irradiated in a flow reactor. Since the TPID/$CHCl_3$ system is the first isothermal photochemical system for which an instability has been observed, it was believed to be important to understand its origin.[18] In the present paper, the instability is understood in terms of a photometric feedback mechanism. One of the key elements of this feedback mechanism is the screen effect of strong light absorbers on weaker ones. The coupling of this screen effect with the acid-catalyzed destruction of TPI• radicals leads to multiple steady states. As a final note, let us emphasize that photochemical kinetics are essentially nonlinear and contrary to chemical kinetics, any given photochemical rate is dependent on the concentration of all light absorbers. Phenomena such as the screen effect are therefore present in even the simpler multicomponent photochemical system.[5] The development of nonlinear photochemical dynamics is however still in its infancy, and much more fundamental work is required before complex instabilities such as oscillations and spatial structures can be predicted and observed in photochemical systems. Some of our recent work in that direction is however promising and shows that photochemical oscillations can easily be obtained by merely adding one simple isomerization reaction to the ABC model.[5,12]

Acknowledgment. J.P.L. thanks the Ministry of National Defence of Canada for supporting this project under Grant No. ARP 3610-644:FUHDS.

Appendix A

1. Determination of Molar Extinction Coefficients at 360 and 554 nm. The molar extinction coefficients of TPID and TPI at 360 and 554 nm were determined with use of analytical solutions of TPID and TPI in chloroform (Table I). The value of $\epsilon_{554}^{TPI•}$ was determined by titrating solutions of TPID/$CHCl_3$, at their photostationary state, with a 0.011 M solution of hydroquinone in ethanol.[4a] Our value of $\epsilon_{554}^{TPI•} = 7000$ L·mol^{-1}·cm^{-1} is slightly lower than the value reported by Maeda and Hayashi, i.e. 8400 L·mol^{-1}·cm^{-1} (in benzene).[4a] In order to determine $\epsilon_{360}^{TPI•}$, we assume that, at the very beginning of the irradiation (in a batch experiment), the only significant light absorbers are TPID and TPI•. At time t_i, we thus have

$$A_\lambda(t_i) = A_\lambda^{TPID}(t_1) + A_\lambda^{TPI•}(t_i) \qquad (A1)$$

where $A_\lambda^j(t_i)$ is the absorbance of species j at wavelength λ and time t_i and $A_\lambda(t_i)$ is the total absorbance under the same conditions. For two absorbance readings at times t_1 and t_2, one can show that

$$\epsilon_\lambda^{TPI•} = \frac{[A_\lambda(t_1) - A_\lambda(t_2)]\epsilon_{554}^{TPI•}}{[A_{554}(t_1) - A_{554}(t_2)]} + 0.5\epsilon_\lambda^{TPID} \qquad (A2)$$

Using λ = 360 nm and the previously determined values of $\epsilon_{554}^{TPI•}$ and ϵ_{360}^{TPID} (Table I), one finds $\epsilon_{360}^{TPI•} = 37\,000$ L·mol^{-1}·cm^{-1}.

2. Determination of I_0. The value of I_0 was determined according to standard actinometric procedures,[9] using benzophenone, under conditions identical with those in Figure 2.

3. Determination of k_2 and k_3. In benzene solutions, the decay rate of TPI• radicals obeys a second-order rate law.[4,7] In chloroform solutions, however, a quantitative analysis reveals that a first-order decay is also significant. This first-order process corresponds to unimolecular reaction R2. In order to determine k_2 and k_3, we consider that for short irradiation times, the only significant decay reactions are (R2) and (R3) such that

$$d[TPI•]/dt = -2k_3[TPI•]^2 - k_2[TPI•] \qquad (A3)$$

The values of k_2 and k_3 were determined simultaneously from a nonlinear best fit of TPI• radical decay curves to (A3).

4. Determination of k_6. The rate of reaction R6 is given by

$$d[TPI•]/dt = -k_6[H^+][TPI•] \qquad (A4)$$

The value of k_6 was determined as follows. Before any irradiation, a known amount of monochloroacetic acid (typically 1.5×10^{-4} M) was added to the TPID/$CHCl_3$ solution. The irradiation was then carried out at 450 nm for a very short period of time (e.g., 15 s). At that wavelength, only TPI• radicals are produced and photolysis of TPI present in the TPID solution is negligible. During the irradiation, a small concentration of TPI• radicals is produced through (R1) ($\simeq 5 \times 10^{-6}$ M). An equivalent small amount of acid is at the same time destroyed through (R6). The latter is however considered to be negligible as compared to the initial amount of acid added. Process R6 is then the main deactivation route and its rate is easily estimated from the decay of the absorbance at 554 nm, at the beginning of the irradiation (initial rate method), viz.

$$k_6 = \frac{[(dA_{554})/dt]_0}{[H^+]_0[A_{554}]_0} \qquad (A5)$$

where $[(dA_{554})/dt]_0$ is the initial decay rate of TPI• radicals after the irradiation is turned off, $[H^+]_0$ is the initial acid concentration, and $[A_{554}]_0$ is the value of the absorbance at 554 nm at the moment the light is turned off. An average over a number of runs gives $k_6 = 524 \pm 50$ L·mol^{-1}·s^{-1}.

5. Determination of ϕ_1. The quantum yield of photoreaction R1 is defined as

$$\phi_1 = \frac{d[TPI•]/dt}{2I_1} \qquad (A6)$$

where I_1 is defined in eq 2. The value of ϕ_1 was evaluated from simultaneous measurements of the absorbances at 360 and 554 nm at the very beginning of the irradiation. Using (2), and the previously determined values of $\epsilon_{554}^{TPI•}$ and I_0 (Table I), one finds $\phi_1 = 0.013 \pm 0.008$.

6. Determination of ϕ_4. The quantum yield ϕ_4 can be expressed as

$$\phi_4 = \frac{d[TPI]/dt}{I_a} \qquad (A7)$$

This quantum yield was determined from the photolysis of a 8.25×10^{-5} M TPI solution in chloroform. The procedure was analogous to the one described above, with $I_a = I_0(1 - 10^{-A_{360}^{TPI}})$. The average obtained over a few runs gives $\phi_4 = 0.0012 \pm 0.0005$.

7. Determination of ϕ_5. This quantum yield is expressed as

$$\phi_5 = \frac{d[H^+]/dt}{I_a} \qquad (A8)$$

Its value was determined according to a procedure similar to eq 6 above, but where the amount of acid liberated per unit time was determined by titrating the solutions with KOH, for increasing irradiation times. The average value found over different experiments is 0.009 ± 0.003.

(18) Multiple steady states have been observed in a variety of nonisothermal irradiated systems. For example, see: Kramer, J.; Reiter, J.; Ross, J. *J. Chem. Phys.* **1986**, *84*, 1492–1499 and references therein.